university of groningen

Modelling and Analysis

Of the pumping system of
the Ocean Grazer under
realistic wave motion

BSc thesis

to obtain the degree of BSc at the
University of Groningen.

Study:
Industrial Engineering and
Management

by

Gerwin Matthijs Loer

born on 12 May 1997
in Delfzijl,

Supervisor
Prof.dr. Jayawardhana

Co-supervisor
Dr. M. Muñoz - Arias

Daily-supervisor
M.Almuzakki,PhD

Assessment committee

Prof. dr. Jayawardhana
Dr. M. Muñoz - Arias

Abstract

In this project, a new concept towards modelling the pumping system of the Ocean Grazer is considered. The Ocean Grazer will be an enormous platform in the sea which is able to harvest energy from incoming sea waves and store it in a reservoir at a higher altitude. The Ocean Grazer is currently in the research and development phase. The validity of the project is under investigation by employees and students of the University of Groningen. This Bachelor Integration Project will extend the knowledge of the pumping system within the Ocean Grazer under realistic wave motion, with as purpose making the Ocean Grazer a viable option to manufacture.

The novel system will have a different representation of the Power Take Off System (referred to as PTO) than previous researches up till this moment in time. The Power Take Off is described by the dynamics of the hydraulic subsystem of the Ocean Grazer. In addition, this project considers accurate representations of the excitation and radiation forces which is not yet combined with the above mentioned novelty in previous researches of the Ocean Grazer Group.

Acknowledgements

First, I would like to thank Prof.dr. Jayawardhana for introducing me with the Ocean Grazer project. He provided me with the opportunity to develop myself by assigning me with this challenging project.

Secondly, I would like to thank M. Almuzakki, PhD and dr. M. Muñoz Arias for their time and effort to guide me through Matlab coding, explanations of the mechanical and hydraulic subsystems in the Ocean Grazer and familiarizing me with the programming language Matlab and in specific Simulink.

Furthermore, the time and effort of all the members of the Ocean Grazer group were much appreciated throughout the entire project.

List of abbreviations

Abbreviations	Full description
EMEC	European Marine Energy Centre
PTO	Power Take Off
TRL	Technology Readiness Level
TW	Terra Watt
GWh	Giga Watt per hour
KJ	Kilo Joule

Nomenclature

Variable	Description	Unit
Ac	Area of the floating element	m^2
Af	Area of the floating element	m^2
$C_{h,r1}$	Fluid capacitance between the higher reservoir and resistor 1	$\frac{kg}{m^4 s^2}$
$C_{r2,l}$	Fluid capacitance between the lower reservoir and resistor 2	$\frac{kg}{m^4 s^2}$
C	Total fluid capacitance system	$\frac{kg}{m^4 s^2}$
E_p	Energy of the pump	J
E_{pot}	Potential Energy generated by the wave extraction	J
F_e	Excitation forces over time	N
$F_{floater}$	Force generated by the motion of the floater	N
F_{pto}	Force generated by power take off systems	N
F_r	Forces generated by the radiation of the other floating elements	N
F_b	Buoyancy forces on the floating element	N
g	Gravitational constant	$\frac{m}{s^2}$
I_1	Fluid inertance at higher part of the mechanical subsystem	$\frac{kg}{m^4}$
I_2	Fluid inertance at lower part of the mechanical subsystem	$\frac{kg}{m^4}$
I	Total fluid inertance of the coupled system	$\frac{kg}{m^4}$
k	Buoyancy spring constant	$-$
L	Length of the water column	m
m	Mass of the floating elements	kg
m_∞	Constant positive added mass	kg
P	Pressure over a section	Pa
P_s	Pressure source of the hydraulic subsystem	Pa
$\dot{P}$	Dynamics pressure difference between both reservoirs	$\frac{Pa}{s}$
Q	Flow rate inside the water column	$\frac{m^3}{s}$
q	Displacement of the pistons	m
$\dot{q}$	Velocity of the pistons	$\frac{m}{s}$
$\ddot{q}$	Acceleration of the pistons	$\frac{m}{s^2}$
$\dot{Q}$	Acceleration of the flow rate	$\frac{m^3}{s^2}$

r_1	Fluid resistance of the first fluid resistor	$\frac{kg}{m^4 s}$
r_2	Fluid resistance of the second fluid resistor	$\frac{kg}{m^4 s}$
R	Total fluid resistance generated by the two fluid resistors	$\frac{kg}{m^4 s}$
z	Displacement of the radiation component (convolution kernel)	m
$\dot{z}$	Velocity of the radiation component (convolution kernel)	$\frac{m}{s}$
φ	Convolution kernel of the radiation forces of the floating elements	$-$
ρ	Density of the water inside the water column	$\frac{kg}{m^3}$
μ	Conditioned fluid dynamical viscosity	$\frac{Ns}{m^2}$

List of tables

List of figures

Table of contents

1 Introduction

1.1 Urgency of renewable energy sources

With the depletion of the energy resources over the foreseeable future, the urgency of the renewable energy resources are awakened. The primary energy resources of the 20th century: coal, gas and oil have an expected life span of less than 150 years (Shafiee and Topal, 2009). These primary energy resources satisfy approximately 80 % of the energy consumption of the entire world. Therefore, new alternative energy resources are needed to be incorporated worldwide, also keeping in mind that the energy demand will increase in the 21th century (Pérez-Lombard, Ortiz and Pout, 2008).This effect is not only stimulated by the fact that more people are able to use energy powered devices but also because of the fact that the population of the earth is increasing drastically (Pérez-Lombard, Ortiz and Pout, 2008).

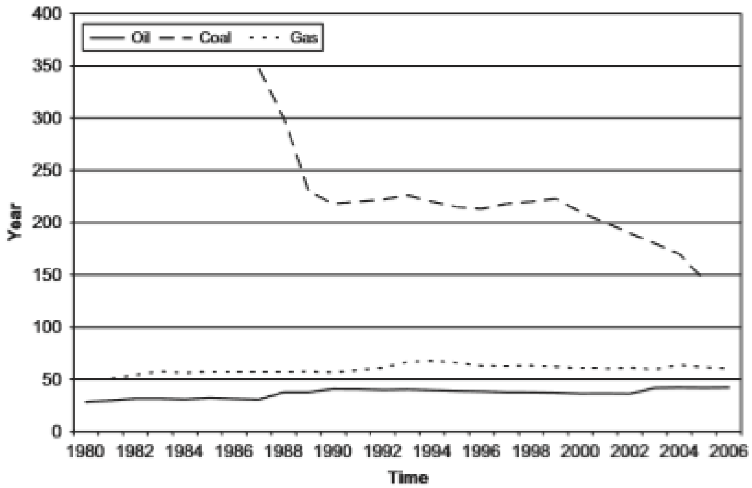

Figure 1: The development of the expected life span of the primary energy resources (Shafiee and Topal, 2009).

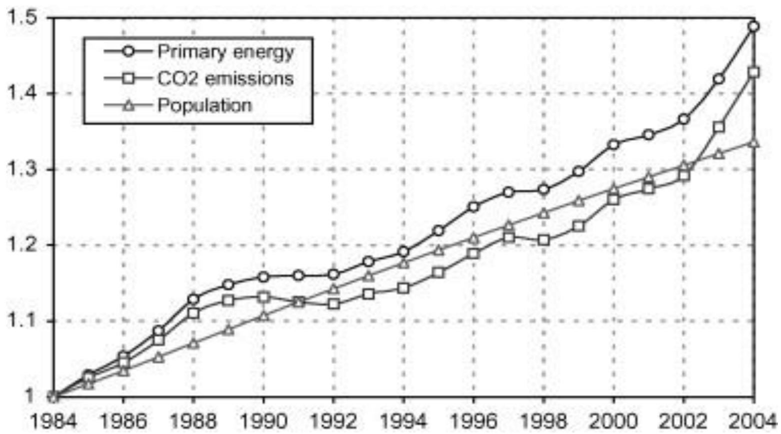

Figure 2: Percentage change of the worldwide energy demand, CO2 emission and population (Pérez-Lombard, Ortiz and Pout, 2008).

The current primary energy resources harm the environment on this planet. Research has shown that there is correlation between CO_2 emission and the production of energy with fossil fuels such as coal, oil and gas. Elevated concentration levels of CO_2 cause the temperature of the earth to increase. Global warming has got many negative influences on both the ecological and economical welfare of the human race.

The conclusion which can be drawn from the previous mentioned statements is that the current way of producing energy must change. It still remains unclear how this can be tackled appropriately. However, the first changes are made in the accumulation of energy. Some of the alternative energy resources have developed rapidly in the last two decades. Examples of these sources are: solar energy, nuclear energy and wind energy.

Although the previous mentioned alternative energy sources are beneficial for tackling the global problem, more energy output will be needed for the coming centuries. Luckily, the earth possesses a substantial amount of energy resources which are till this moment in time underdeveloped by the human species. The best example is water energy. In specific energy extraction from oceanic waves. Oceanic Waves carry large amounts of energy. The drawback of wave energy is that only two percent of the coastal waters is powerful enough to be extracted (Jacobsen, 2009). Therefore, devices are needed to be placed off shore, which raises several difficulties. These will be evaluated in paragraph 1.2.

Currently, at the University of Groningen, a research unit is developing a device which is able to extract energy from waves with a plant, that will be based off- shore. This device is called the Ocean Grazer. More information about Wave Energy Converters and the Ocean Grazer will be outlined in paragraph 1.2 & 1.3.

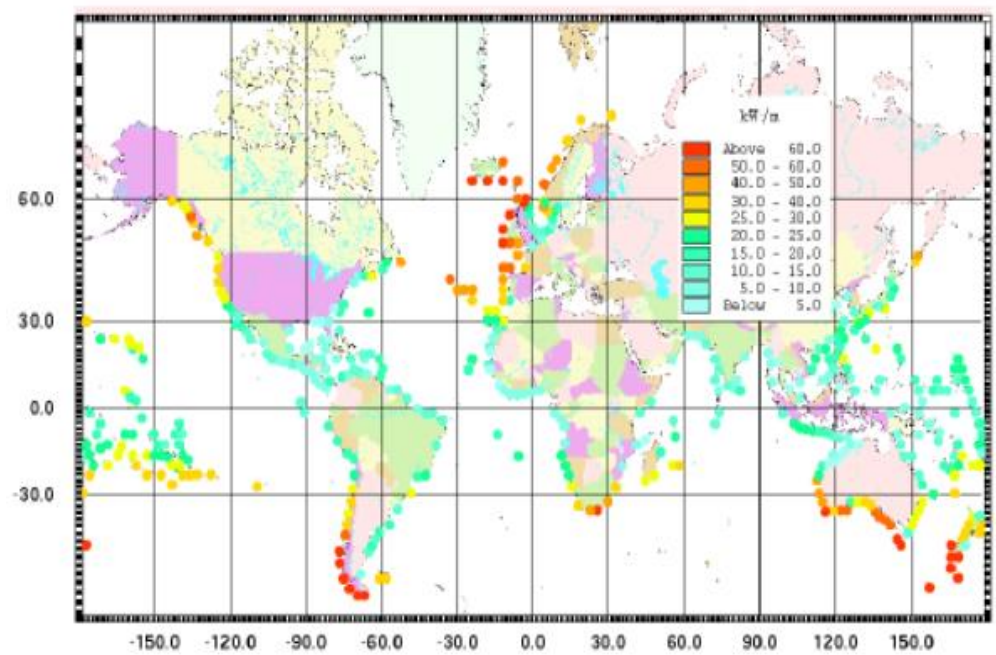

Figure 3: Global distribution of oceanic wave energy (Barstow et al.,1998)

1.2 Wave energy converters

Energy which is harvested from oceanic waves, is called wave energy. Wave energy is harvested with the use of Wave Energy Converters (WEC). WECs are distinguished based upon the technical focus or the location of the WEC (Drew, Plummer and Sahinkaya, 2009), (Yu, 2017), (Falnes and Løvseth, 1991) (European Marine Energy Centre, 2018)).

Wave energy converters can be based at three different locations. These locations are stated and explained down below.

- Possible locations of WECs

  - **On-Shore**: The WEC will be positioned on the shore. The cost will be lower due to lower transportation, maintenance and installation costs. The disadvantage however of On-Shore WECs is the lower potential energy of the sea waves near shore which reduces the energy source. As the water depth decreases, energy is lost by friction at the sea bed and wave breaking occurs on shallow water. Furthermore, as mentioned in paragraph 1.1 there is a limited amount of coast lines which are suitable for wave energy extraction.
  - **Near-Shore**: The WEC will be placed in the sea, near the shore. There are similarities with the On-Shore placement advantages and disadvantages. The cost will be higher to place a WEC near-shore however the benefits regarding energy extraction will also be higher.
  - **Off -Shore**: The WEC will be placed off-shore. The costs will be the highest, maintenance and installation of the site will be difficult to perform, while the benefits are the highest. Another point of discussion is the visual impact of WECs. The visual impact seen from the land will be limited for off-shore devices while on-shore WECs can harm the visual environment for inhabitants in the neighborhood of the WECs.

Besides different locations, the technical focus of a Wave energy converter can be used as a differentiation factor. Therefore, these WECs can be differentiated from each other based on the criteria down below. This research is limited to the Ocean Grazer WEC. Each of the technical focuses included in the Ocean Grazer WEC will be highlighted by the following symbol:*.

- Technical Focus

  - **Point Absorber Buoy ***: A floating buoy attached with an cable or rod follows the motion of incoming sea waves. The cable follows the motion of buoy/sea wave. The cable can actuate pumping systems, where after pumps can transform the energy into other useful forms for instance potential energy.
  - **Attenuator***: The attenuator is a floating device in the sea which follows the motion of the sea waves. The attenuator extracts its energy from the relative motion of the two arms as the waves passes them.

- **Oscillating wave surge converter**: is a device in the sea which is able to extract energy from wave surges and moving water particles within water surges. The arm oscillates as a pendulum mounted on a pivoted joint in response to the movement of water in the waves.
- **Oscillating water column ***: An oscillating water column is a partially submerged, hollow structure. It is open to the sea below the water line, enclosing a column of air on top of a column of water. Waves cause the water column to rise and fall, which in turn compresses and decompresses the air column. This trapped air is allowed to flow to and from the atmosphere via a turbine, which usually has the ability to rotate regardless of the direction of the airflow. The rotation of the turbine is used to generate electricity.
- **Overtopping/terminator device**: Overtopping devices capture water as waves break into a storage reservoir. The water is then returned to the sea passing through a conventional low-head turbine which generates power. An overtopping device may use ‘collectors’ to concentrate the wave energy. Overtopping devices are always based near shore.
- **Submerged pressure Differential**: This device is normally positioned near to the shore and attached to the seabed. The motion of the waves create pressure differences by constantly changing the water level above the device. The pressure difference can actuate a pumping system to generate electricity.
- **Bulge wave**: Bulge wave technology consists of a rubber tube filled with water, moored to the seabed heading into the waves. The water enters through the stern and the passing wave causes pressure variations along the length of the tube, creating a ‘bulge’. As the bulge travels through the tube it grows, gathering energy which can be used to drive a standard low-head turbine located at the bow, where the water then returns to the sea.
- **Rotating Mass**: The rotating mass makes use of two degrees of freedom, the heaving and swaying motion . The device can transform the motion into useful energy by an electric generator inside the device. The transformation of motion is done by either an eccentric weight or a gyroscope. This is done to generate precession.
- **Upcoming inventions:** according to EMEC there are new developments to create new types of WECs in the near future. Examples are the Wave Rotor, which is able to directly use the waves as input to actuate the turbine. Other developments are on flexible structures, where the shape or volume of the power take off system change over time or input.

1.3 Ocean Grazer

The Ocean Grazer could be the new energy resource of the future. The Ocean Grazer will be an enormous platform in the sea (The structure itself has a diameter of 435 meters and a height of 255 meters, of which 30 meters is situated above the ocean surface (oceangrazer.com)), which allows the Ocean Grazer to have room for wind turbines and photovoltaic systems at the surface of the device. The aforementioned energy generators will approximately produce 20 % of the entire energy generation. The remainder of the energy production will be generated by extracting the energy of incoming oceanic waves. Therefore, the main energy source of the Ocean Grazer is the energy of the incoming wave motion. The device is equipped with a multi-piston-power-take-off, this system is able to adapt itself to extract energy in an efficient manner from wave heights varying between one and twelve meters and wave periods between 4 and 20 seconds. The estimated output of a single Ocean Grazer device is 260 GWh per year, approximately 70000 households could be provided with an single Ocean Grazer (oceangrazer.com).

The Ocean Grazer is still in early development stages. The project is currently situated in the fourth phase of the Technology Readiness Level (also referred to as TRL). The TRL categorizes technological development based upon progress made in the project. The TRL is commonly used in engineering and science projects, most famous user is probably the NASA. The research unit of the Ocean Grazer aims with additional research of students and staff members to reach TRL-8. The Ocean Grazer will be launched for production after achieving this target (oceangrazer.com).

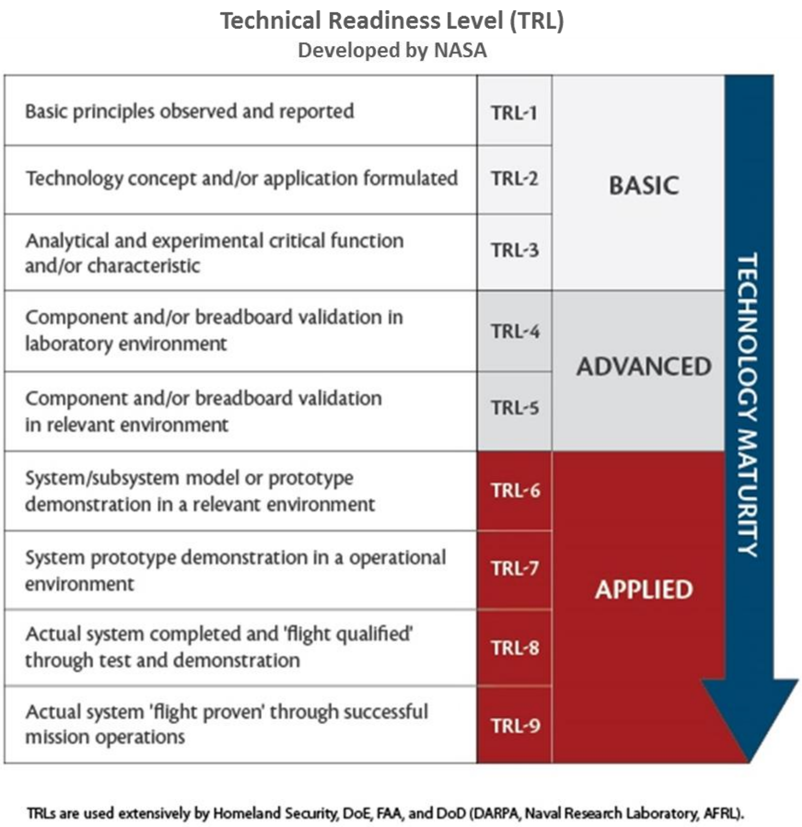

Figure 4 TRL levels explained according to NASA standards (Redstone.us.com)

1.4 Problem owner analysis

Studies about the Ocean Grazer and its development are done at the University of Groningen. However, the Ocean Grazer has recently become a company. Therefore, this company can be seen as problem owner on a higher level (research team of the Ocean Grazer, often referred to as Ocean Grazer Group in this report). Throughout the design phase there will be extensively contact between the problem owner and the designer, in order to meet the specifications and achieve maximum result. The problem owner has all incent to make this research a success which consequently means that the problem owner will support the research if possible.

The Ocean Grazer Group is too general to state as problem owner of this specific problem. Therefore, the supervisors of this project (Prof.dr.Jayawardahana, M.Almuzakki,PhD and dr. M. Muñoz –Arias) are considered to be the main problem owners of this problem, for the reason that they have been involved with researches regarding the pumping system or correlated research. In (Almuzakki et al., 2017) a mathematical model was designed of the dynamics of the floater blanket, which has high correlation with this research. M.Almuzakki,PhD is a researcher in the Ocean Grazer Group, working on the optimization of the PTO system of the floater elements. This research could give him new insights to continue his research. Furthermore, Prof.dr.Jayawardhana and dr.Muñoz-Arias have recently been involved with researches regarding the Ocean Grazer.

1.5 Stakeholder analysis

The first stakeholder which is considered is the Ocean Grazer Group (see: Appendix C). The Ocean Grazer Group is a research unit which focuses on the development of the Ocean Grazer. All members of the Ocean Grazer Group are employees of the University of Groningen, in specific the ENTEG department. Although interest is rising for the Ocean Grazer which can make this research beneficial for similar manufacturers of WECs (wave energy converters) in the future, the information generated in this research will be mainly applicable for the Ocean Grazer Group, because this specific device differs a lot from other WECs. Furthermore, the Ocean Grazer recently received a patent, the research unit is transparent about their project (rug.nl). The research team visits conferences to pitch their ideas and to gain new knowledge regarding wave energy extraction. Furthermore, breakthrough information is published to attract investors and students who want to improve the Ocean Grazer.

Secondly, dr.M. Muñoz Arias, Prof.dr. Jayawardhana and M.Almuzakki,PhD can be seen as stakeholders, because of the fact that they have more direct influence on this bachelor integration project than being regular members of the Ocean Grazer Research Team. Besides that their own researches for the Ocean Grazer are closely related to this specific subject of the Ocean Grazer, they are stated as supervisors in the stakeholder analysis (fig.7).

Thirdly, the partners of the Ocean Grazer Group have got a stake in the outcome of this research. The University of Groningen for instance funds research of the Ocean Grazer. In addition, the university will receive positive publicity when the project will become successful. (Academic) Network Partners will also be influenced by this research due to increased publicity. Besides the increased publicity the knowledge base of these institutes altogether will increase due to the extensive collaboration .

The Ocean Grazer Network is a collaboration between companies, government bodies, organizations and research institutes that have declared active support and a principal willingness to participate in the further development of the Ocean Grazer. Network members will be invited to participate in specific research proposals, depending on their area of expertise. (Oceangrazer.com)

Figure 5: Network Partners of the Ocean Grazer Group (Oceangrazer.com)

Figure 6: Academic Network Partners of the Ocean Grazer Group (Oceangrazer.com)

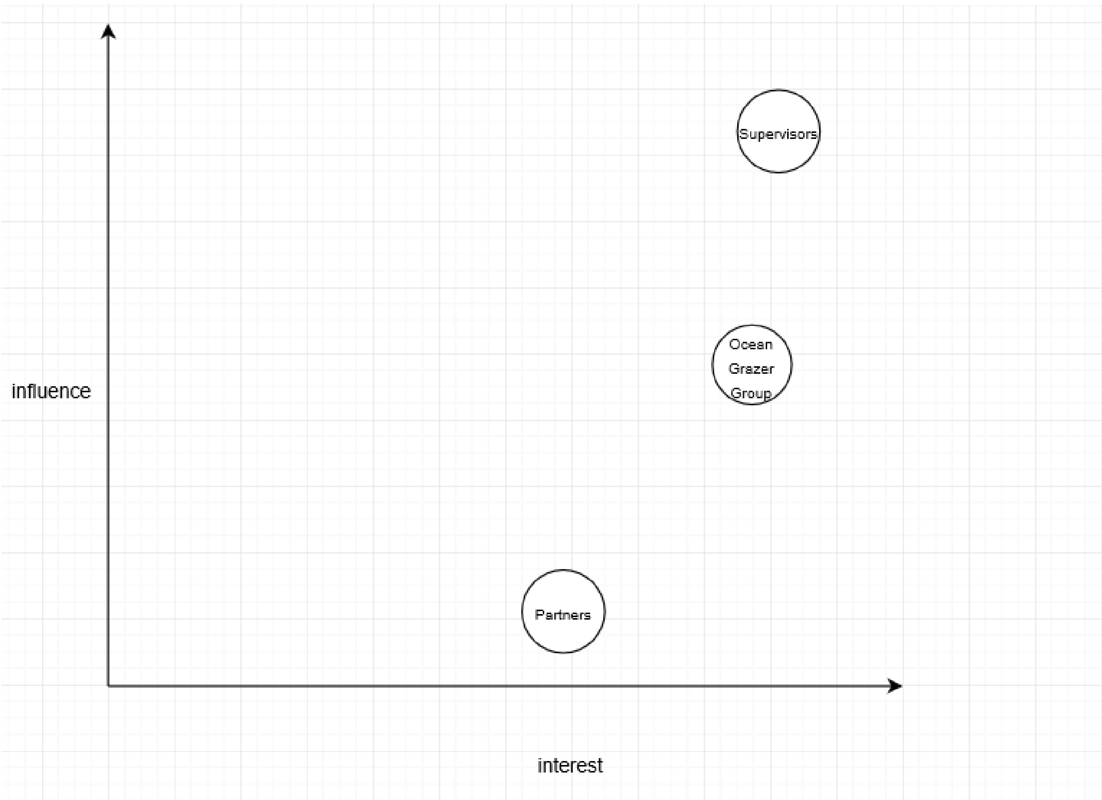

Figure 7: Stakeholder analysis.

1.6 Goals of the project

Previous work of (Almuzakki et al.,2017) has shown the effect of Linear PTO on the floater arrays of the Ocean Grazer. In (Almuzakki et al.,2017) the equations of motion of the mechanical subsystem of the Ocean Grazer were introduced. Besides the equations of motion of the mechanical side, the paper includes the radiation forces and excitation forces acting on the floater elements. In (Almuzakki et al.,2017) future work was mentioned. The aforementioned future work consists of the integration of the PH model of the multi-floater system with the non-linear PTO systems of the Ocean Grazer WEC and use it to optimize the power generation of the device. Although this research has some differences, the proposed work is partly evaluated in this research. The energy generation for instance is calculated with influences of non- linear PTO.

This bachelor integration project will use the mathematical model of (Almuzakki et al.,2017) and adapt the mathematical model with the influences of non-linear PTO to visualize the pumping behaviour of the OG WEC. This will be done by using the mechanical subsystem which is used in (Almuzakki et al.,2017) and combining it with the hydraulic subsystem mentioned in (Barradas-Berglind et al.,2017). The novelty of this research is combining the influences of non-linear PTO, radiation forces, excitation forces and buoyancy (restoring) forces in one single mathematical model to simulate the behaviour of the Ocean Grazer, in specific the pumping system. This research aims to represent the pumping behaviour under realistic wave motion as accurate as possible in order to create more insight in this process for the problem owner.

1.7 Research questions

In paragraph 1.6 it was stated that the pumping system was not yet modelled under realistic wave motion with all parameters used in (Almuzakki et al.,2017). Therefore, with this knowledge the following main research question was determined.

1.7.1 Main research question

What will be the behavior of the Ocean Grazers pumping system under realistic wave motion?

The main research question will be solved by answering initial research questions. Therefore, the following initial research questions were described.

1.7.2 Other research questions

- How to model irregular wave motion in a mathematical model?
- How will the pumping behavior differ under realistic wave motion in comparison to linear wave dynamics?
- How to describe the realistic power take off system mathematically?

1.8 Methodology used in this project

This research will be based upon the three cycle approach of Hevner. The three cycles are denoted as: the relevance cycle, the design cycle and the rigor cycle. The relevance cycle is used to draw the requirements and demands from the problem owners. The design cycle is used to create and evaluate the new mathematical model. Finally the rigor cycle is used to adapt all the available knowledge of previous research and extend the knowledge base.

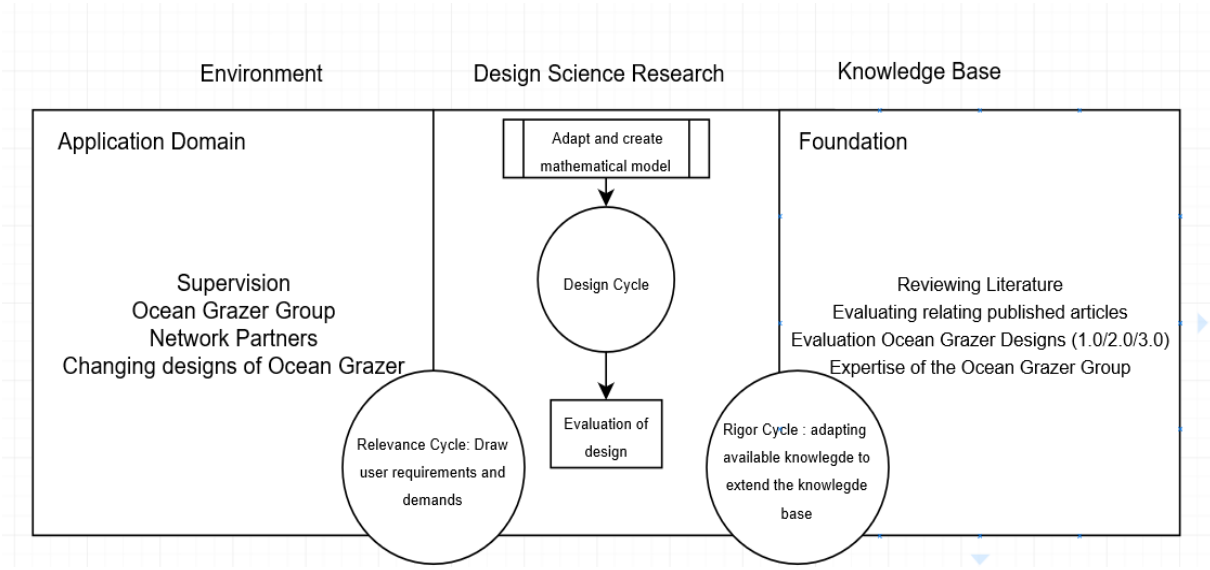

Figure 8: Hevner three cycle approach specified to this problem.

The goal of this project was to achieve more insight in the pumping behaviour under realistic wave motion, mathematical modelling was used to fulfill this goal. The system was considered as a hard system, because of the limited influence of human interaction in the entire research. Apart from the interaction between designer and supervisors/stakeholders, there is actually no signs of soft elements.

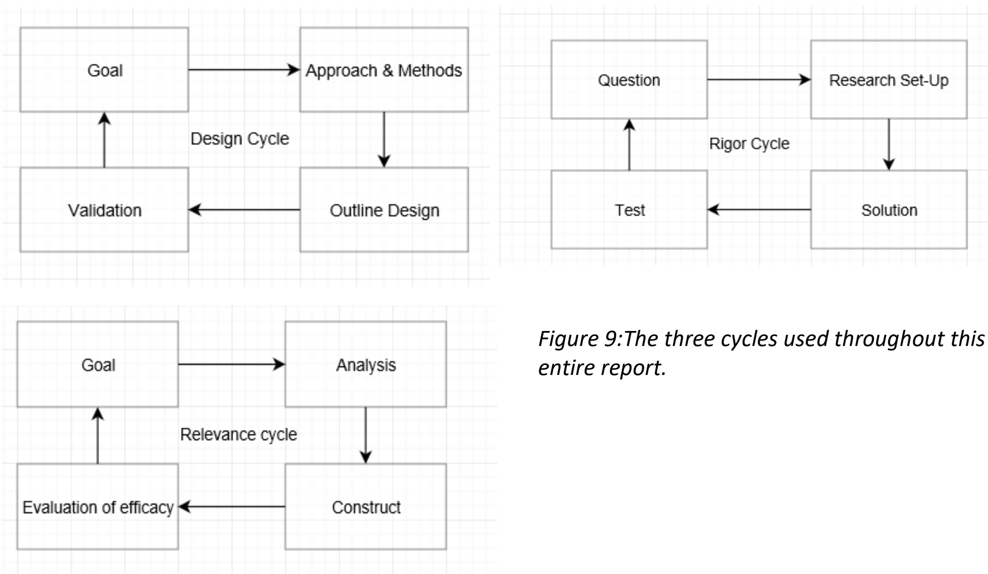

Figure 9:The three cycles used throughout this entire report.

Besides the aforementioned importance of the relevance cycle, the relevance cycle was also used to describe the system description and the boundaries for this research. The designer and the problem owners had intensive contact throughout the research, the relevance of each component of the pumping system was evaluated in consent. The design cycle was used throughout this research because of the importance of the mathematical model and the design steps in the way towards this model. The design cycle however was approached in a bit of different way, this because the validation of the mathematical model was performed in smaller steps. The mathematical model was each time made more complex by adding a new variable to the model. After each individual step the mathematical model was run in order to check whether the model was working without errors.

1.9 Scope and assumptions

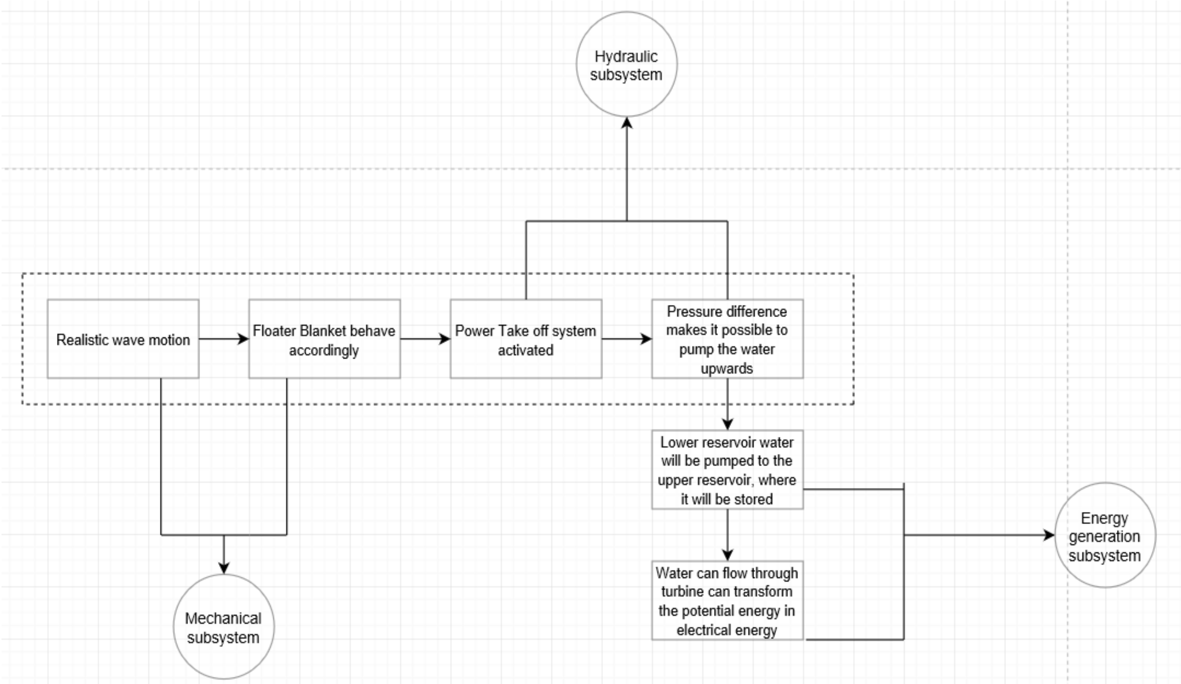

Figure 10: Shortened System Description from the Ocean Grazer (dashed line the scope of this research).

The system description of the Ocean Grazer can be divided in to three subsystems. The three subsystems can be identified as: the hydraulic subsystem, the mechanical subsystem and the energy generation subsystem. The first two subsystems are considered in this research. The generation and transformation of the energy is not incorporated in this research because of the limited correlation with the pumping behaviour of the Ocean Grazer. It is assumed throughout the research that the efficacy between the first two subsystems and the energy generation subsystem is optimal. This means no leakage of energy or losses in the system. This assumption is made when describing the energy of the system. This research contains all the relevant elements of the Ocean Grazer until the water is pumped up to the higher reservoir.

The mathematical model created in this research is based upon a single floater element, this means that all the variables which were obtained from other research teams of the Ocean Grazer were adapted such that they will comply with this assumption. The conditions within the hydraulic subsystem are taken to be exactly the same as in (Barradas-Berglind et al.,2017). This means that the fluid capacitance, fluid densities, fluid resistance, length of the water column and the areas of the floater elements will be exactly the same. (values of each of these components are visible in paragraph 4.1) Furthermore, the areas of the pistons are in reality adaptable to the wave input, but in this research one of the seven options is chosen to be a constant throughout all the simulations.

The radiation force, excitation force and the wave input were directly obtained from work in progress of M.Almuzakki,PhD and R.J.Boer. The buoyancy force was calculated on exactly the same way as mentioned in (Almuzakki et al.,2017). The displacement of the waves and the displacement of the pistons are taken to be equal to each other, this also counts for all the correlated variables, for instance the derivative and the second derivative (velocity and acceleration). This is done to be able to calculate the coupled system. Although, in reality these displacements could slightly differ.

$$q_{floater} = q_{waves} \tag{1}$$

2 Theoretical Framework

2.1 Existing knowledge base related to the pumping system

The Ocean Grazer Group has performed research on the pumping behaviour in previous published papers. In (Barradas-Berglind et al.,2017) a modular design of the hydraulic subsystem in combination with a moving water body/ piston-buoy ensemble was considered. In this research the incoming wave was considered to be a linear wave input. The radiation forces and excitation forces were not included in the description of the dynamics between the switched buoy piston ensemble and the pumping system. This research is the foundation of the hydraulic subsystem described in paragraph 2.4.

In (Almuzakki et al.,2017) the dynamics of the mechanical subsystem were described with a linear Power Take Off system. In this research the radiation forces were described according to the NEMOH toolbox which was first introduced by Babarit and Delhommeau in 2015. This toolbox makes it possible to transform the geometry of the floating elements in a convolution kernel (φ). The linear PTO being considered was modelled by a damper and a spring with positive constants. The buoyancy force or restoring force was represented by a spring system, in which the considered spring constant was equal to the buoyancy constant. (Almuzakki et al.,2017) is primarily used to represent the mechanical subsystem described in paragraph 2.5.

In (Vakis et al.,2016) the mechanical design and model of a single piston pump was presented for the first time. Similarly to the previous mentioned researches, this research is based upon a sinusoidal wave input which simplifies the calculations. However, differences are the representation of the excitation force and the exclusion of the radiation forces of the floater elements. The excitation force was represented by a numerical approximation based on pressure, inertial and damping contributions.

Anno 2018, M.Almuzakki,PhD and R.J.Boer are developing a mathematical model which is able to create more insight in the behaviour of the floater blanket of the Ocean Grazer. Improvements to the model created by M.Almuzakki,PhD in 2017 is the increased number of floater elements considered and the influence of irregular wave motion in the mathematical model. The representation of the radiation forces and the excitation forces were directly obtained from this new research which is not yet published.

2.2 Port – Hamiltonian approach & State Space representation

The Port-Hamiltonian approach and State Space representation are commonly used by researchers of the University of Groningen to represent the dynamics of the Ocean Grazers subsystems. In this paragraph, more background information will be stated to simplify the adoption of the coming information outlined in the next paragraphs. Although the Port-Hamiltonian framework will not be used in this report, it is useful to give background information because information is extracted from researches based upon this approach. Furthermore, it simplifies the transition to read other relevant researches from the Ocean Grazer Group.

The Port-Hamiltonian approach was introduced in 1992 by Prof.dr. van der Schaft. The Port-Hamiltonian description offers a systematic framework for analysis, control and simulation of complex physical systems, for lumped-parameter as well as for distributed-parameter models. The Ocean Grazer is usually described by a lumped-parameter model which makes the Port-Hamiltonian approach a valid option to describe the dynamical behaviour of the Ocean Grazer.

The PH-framework consists of a representation of the system in terms of energy variables, their interconnection structure and power ports. Systems which are represented in the PH-framework include large families of physical non-linear systems. The transfer of energy between physical systems and the environment is given through energy elements, dissipation elements, and power preserving ports. For more information about the PH-framework see: (Barradas-Berglind et al.,2017), (Maschke and van der Schaft,1992),(van der Schaft,2000) and (Duindam et al.,2009).

The Port-Hamiltonian Approach is represented by

$$\dot{x} = \lfloor J(x) - R(x) \rfloor \frac{\partial H(x)}{\partial x} + g(x)u \tag{2}$$

$$y = g(x)^T \frac{\partial H(x)}{\partial x} \tag{3}$$

with states $\epsilon\ \mathbb{R}^{n*n}$, skew-symmetric interconnection matrix J (x) $\epsilon\ \mathbb{R}^{n*n}$, positive semi-definite damping matrix R(x) $\epsilon\ \mathbb{R}^{n*n}$, and Hamiltonian H (x) ϵ . The matrix g (x) $\epsilon\ \mathbb{R}^{n*m}$ weights the action of the control inputs u $\epsilon\ \mathbb{R}^{m}$ on the system, and (u,y) $\epsilon\ \mathbb{R}^{m}$ with M≤N, form a power port-pair.

The State Space representation was introduced in the early 1950s by Richard Bellman. (Kalman and Kalaba,1965). The State Space representation normally shows the minimal amount of physical variables (state variables) to describe the dynamical behaviour of the system. The State Space representation is used to describe the behaviour of differential equations. Describing a dynamical system with state variables simplifies the system especially for computers. Therefore it is suitable for the mathematical model later on in the research.

The State Space is usually represented by

$$\dot{x} = Ax + Bu \tag{4}$$

$$y = Cx + Du \tag{5}$$

and the variables of these equations are denoted by

Element of the State Space	Description
Matrix A	State matrix
Matrix B	Input matrix
Matrix C	Output matrix
Matrix D	Feedforward matrix
U	Input vector
X	State vector
Y	Output vector
$\dot{x}$	Differentiation of state vector

Table 1: State Space model elements

2.3 Oceanic waves and its properties

Waves are generated by blowing winds. Sea swells transport energy from storm centres to distant shores.(Falnes, J. and Løvseth, J. (1991). Previous statistical research has shown the energy levels which can be reached at different oceanic regions. At latitudes between 40 degrees and 65 degrees the energy levels can reach 100 KW/m. When approaching either the equator or both of the poles the energy levels decrease (Falnes, J. and Løvseth, J. (1991)). The total possible energy which can be extracted from waves globally is around 10 TW (Falnes, J. and Løvseth, J. (1991)). However,the energy levels can vary substantially over time. The average possible wave energy can vary a factor 10 from one week to the next week. This increases difficulties for the WECs to predict the input of wave motion in order to set the parameters of the device to optimize the energy extraction.

Waves are usually represented by sinusoidal functions in mathematics, however the behaviour of realistic waves differs from this approximation. Realistic waves are influenced by variables which change over time. Examples of these variables are changing forces of wind power, depth of the ocean or sea, position and geometry of the coastline. (Young, 1999).

This research used the datasets from previous research of the Ocean Grazer group. The realistic wave motion was represented by the eta.dataset , which is incorporated in the excitation force with the following relationship

$$F_e = \varphi eta. dataset \tag{6}$$

The convolutions kernel describes all of the external excitation forces which act on the system. The excitation force was directly obtained from a dataset from M.Almuzakki,PhD. This means that both the convolution kernel, as the dataset were directly obtained from M.Almuzakki,PhD.

2.4 Hydraulic subsystem of the Ocean Grazers pumping system

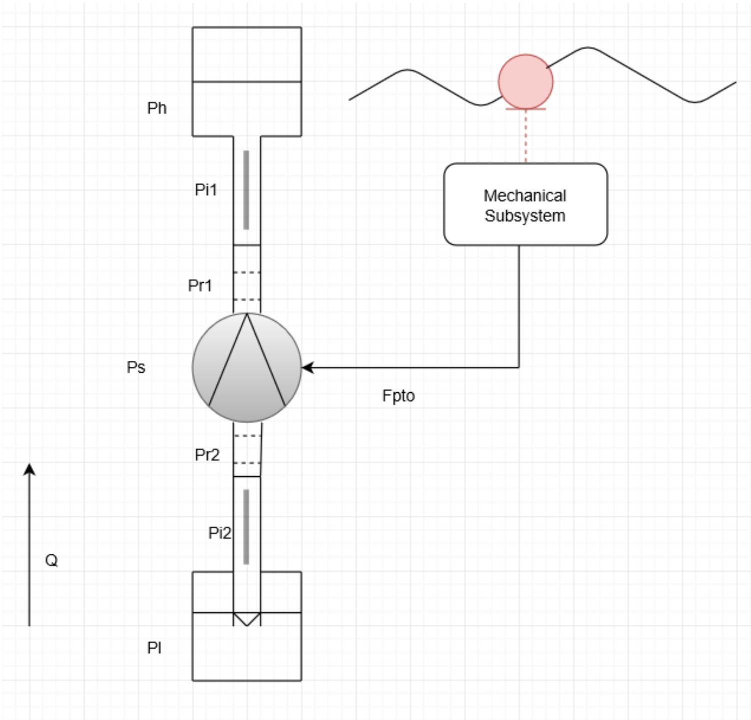

Figure 11: Visualization of the hydraulic subsystem and the relationship with the mechanical subsystem

The hydraulic subsystem of the Ocean Grazer consists of: a pressure source, two fluid resistors, two fluid inertors, check valve and two reservoirs (upper and lower). The purpose of the check valves are depended on the movement of the pistons. If there is upstroke inside the pistons then the internal valves are closed and the water inside the water column can be displaced upwards. On the other side if there is down stroke inside the pistons then the valves are open to allow fluid to reach the fluid column, this is done to eliminate the pressure difference between the upper part of the Pumping source and the lower part of the pressure source. Otherwise, the pumping behaviour will be negated during the down stroke.

Concluding from the first subsection, the check valve influences the behaviour of the pumping system. The velocity of the pistons has got a direct correlation with the check valves. The check valves regulate the flow of the water and velocity of the pistons. Therefore, the check valve influences the dynamical behaviour of the pumping system and the energy generated by pump.

The dynamics of the hydraulic subsystem is used to describe the realistic power take off force which will be used when the hydraulic and mechanical subsystem will be coupled.

The dynamics of the hydraulic subsystem where derived from the elemental equations of each separate element, with the use of fluid systems equations.
The elemental equations of the separate components of the hydraulic subsystem are stated down below.

The elemental equation of a fluid inertor is given by

$$P = I\frac{dQ}{dt} \tag{7}$$

The elemental equation of a fluid resistor is given by

$$P = RfQ \tag{8}$$

The elemental equation of a fluid capacitor is given by

$$Qf = Cf\ \frac{dP}{dt} \tag{9}$$

in which P is the pressure over two points, Qf is the volume rate of flow, Cf is the fluid capacitance, Rf is the fluid resistance and I is the fluid inertance.
To satisfy the compatibility law all the pressure drops around a loop must be equal to zero, when applying this to the hydraulic subsystem the following equations can be expressed

$$P_s = P_{i1,r1} + P_{i2,r2} + P_{i2,l} + P_{i1,h} + P_{l,h} \tag{10}$$

when applying the first three equations denoted at the previous pages on the specific intersections seen at (fig.11). The following equations can be expressed

$$P_{i1,r1} = r_1 Q \tag{11}$$

$$P_{i2,r2} = r_2 Q \tag{12}$$

$$P_{i2,l} = I_2\frac{dQ}{dt} \tag{13}$$

$$P_{i1,h} = I_1\frac{dQ}{dt} \tag{14}$$

However, the gravitational influences in the water column are neglected in (11) till (14).
The gravitational influences are given by

$$\mathrm{G} = gL\rho \tag{15}$$

where ρ is the density of the fluid inside the water column, L is the specific length between the components and g is the gravitational constant. When applying (15) to each of the pressures over the selected points the following expression can be derived

$$P_{i1,r1} = r_1 Q + gL_{i1,r1}\rho \tag{16}$$

$$P_{i2,r2} = r_2 Q + gL_{i2,r2}\rho \tag{17}$$

$$P_{i2,l} = I_2\frac{dQ}{dt} + gL_{i2,l}\rho \tag{18}$$

$$P_{i1,h} = I_1\frac{dQ}{dt} + gL_{i1,h}\rho \tag{19}$$

The length between the higher and lower reservoir can be expressed as

$$L_{l,h} = L_{i1,h} + L_{i1,r1} + L_{i2,r2} + L_{i2,l} \tag{20}$$

The total fluid inertance and total fluid resistance can easily be expressed as

$$R = r_1 + r_2 \tag{21}$$

$$I = I_1 + I_2 \tag{22}$$

The fluid inertance was based upon research of (Barradas-Berglind et al.,2017)

$$I_1 = I_2 = \frac{\rho L_{l,h}}{4Ac} \tag{23}$$

Following (Barradas-Berglind et al.,2017), the fluid resistance can be expressed with the use of the Hagen-Poiseuille equation

$$r_1 = r_2 = \frac{2\mu\pi L_{l,h}}{Ac^2} \tag{24}$$

the dynamics of the pressure $\dot{P}$ is given by the difference in pressure between the upper and lower reservoir and is a function of the flow rate Q and both Capacitances before and after the pressure source. However, first the capacitance will be outlines where after in the dynamics of the pressure are given

$$(C_{h,r1}\ ) = \frac{Au}{\rho g} \tag{25}$$

$$(C_{r2,l}\ ) = \frac{Al}{\rho g} \tag{26}$$

$$C = \frac{C_{h,r1}C_{r2,l}}{C_{h,r1} + C_{r2,l}} \tag{27}$$

$$\dot{P} = \frac{Q}{C} \tag{28}$$

As previously mentioned, if the velocity inside the pistons is negative then the pressure inside the pumping system should be zero. Therefore the following expression acts

$$if\ \dot{q} < 0$$

$$\dot{P} = 0 \tag{29}$$

The dynamics of the pressure are otherwise positive which ultimately means after coupling with $Q = Ac\dot{q}$ that the dynamics of the pressure are denoted as

$$if\ \dot{q} \geq 0$$

$$C\dot{P} = Ac\dot{q} \tag{30}$$

When combining (10) up till (28) the following expression for the differential equation of the flow rate can be obtained

$$I\frac{dQ}{dt} = -P_s + RQ + g\rho L_{l,h} + P_{l,h} \tag{31}$$

This expression will be used with the coupling mechanism later on in this report to describe the behaviour of the coupled subsystems. More information about the values and equations used in the mathematical model is outlined in table 2.

2.5 Mechanical subsystem of the Ocean Grazers pumping system

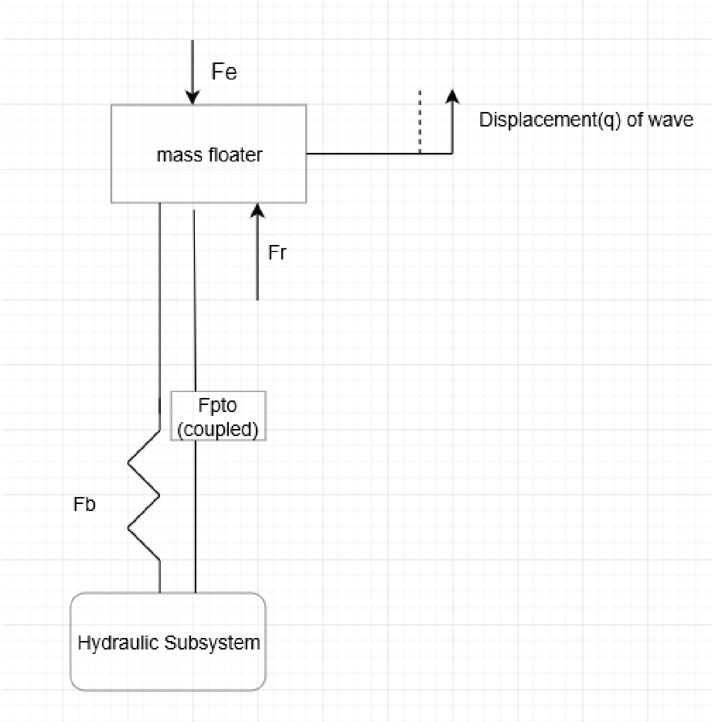

Figure 12 Mechanical subsystem of a single floater within the Ocean Grazer

The mechanical subsystem is represented by all the elements which influence the behaviour of the floating element within the floater blanket. The following elements influence the mechanical subsystem: radiation forces, power take off forces, buoyancy forces and the excitation forces. The buoyancy force is represented by a spring which is activated by the displacement of the buoy. F_{pto} is described via a coupling mechanism with the hydraulic subsystem mentioned in paragraph 2.4. The mechanical subsystem (fig.12) can be represented by the following equation

$$F_b + F_f = F_e + F_r - F_{pto} \tag{32}$$

The radiation force is denoted by the negative added mass of the moving water body multiplied with the motion of the floater and the addition of an radiation integral which was obtained from the NEMOH toolbox. Throughout this research it is assumed that this data is existing knowledge and will not be derived any further.

$$F_r = (-m_\infty)\ddot{q}(t) + \int_0^t \varphi(t-\tau)\dot{q}(t)d\tau \tag{33}$$

The buoyancy force was calculated based upon (Almuzakki et al.,2017), it is represented by a spring system. The spring coefficient is given by

$$K_b = \rho g A f \tag{34}$$

Now the buoyancy force can be expressed as

$$F_b = K_b q(t) \tag{35}$$

The equation of motion simply follows by the acceleration of the wave multiplied by the mass of the floating element. Thus, the force of the floater can be expressed as

$$F_f = m\ddot{q} \tag{36}$$

With the use of a coupling mechanism, (31) could be rewritten to the following form

$$F_{pto} = -Ac\left(IAc\ddot{q} + RAc\dot{q} + g\rho L_{l,h} + P_{l,h}\right) \tag{37}$$

$$Coupling\ mechanism\ : Q = Ac\dot{q} \tag{38}$$

Changes to the overall equation of the mechanical subsystem need to be made to couple both systems. The radiation force will be split into two parts, the added mass will be transferred to the left side of the equation, and the radiation component will be left at the right hand side of the equation. This integral can be changed to a State Space representation which will be outlined in equations down below. However, first the overall dynamical equation will change to

$$(m + m_\infty)\ddot{q}(t) \ = Fe + \int_0^t \varphi(t-\tau)\dot{q}(t)d\tau + Ac\left(IAc\ddot{q} + RAc\dot{q} + g\rho L_{l,h} + P_{l,h}\right) - kq(t) \tag{39}$$

where the radiation integral is represented by

$$\dot{z} = A_{rz} + B_{rz} \tag{40}$$

$$F_r = C_{rz} + D_{rz} \tag{41}$$

With the following properties of the State Space model

$A_{rz} \in \mathbb{R}^{n*n}, B_{rz} \in \mathbb{R}^{n*1}, C_{rz} \in \mathbb{R}^{m*n}\ and\ D_{rz} = 0$ with $m \leq n$.

2.6 Coupled system in the State Space representation

The mechanical subsystem and the hydraulic subsystem are related to describe the realistic pumping behaviour of the pump of the Ocean Grazer under realistic wave motion. The hydraulic system describes the power take off forces due to the changing pressures in the hydraulic subsystem. The changing pressures cause the system to act like a switching system. The power take off is dependent on the wave motion, if the velocity of the wave is positive, then the pump is activated and is able to pump, otherwise the pump is deactivated. This effectively means that the coupled system in state space has got two different representations, namely "switched on" and "switched off". The mechanical subsystem showed the overall equations of the Ocean Grazers pumping system. The combined system is represented in the State Space equations down below (39). The switched off state space model is also based upon (39). However, the PTO force is excluded when the velocity becomes below zero.

$$when\ \dot{q} \geq 0$$

$$\begin{bmatrix} \dot{q} \\ \ddot{q} \\ \dot{z} \end{bmatrix} = \begin{bmatrix} 0 & 1 & 0 \\ \frac{-k}{m+IAc^2} & \frac{-RAc^2}{m+IAc^2} + \frac{D_{rz}}{m+IAc^2} & -\frac{C_{rz}}{m+IAc^2} \\ 0 & B_{rz} & A_{rz} \end{bmatrix} \begin{bmatrix} q \\ \dot{q} \\ z \end{bmatrix} + \begin{bmatrix} 0 \\ \frac{1}{m+IAc^2} \\ 0 \end{bmatrix} (F_e + G) \tag{42}$$

$$y = \begin{bmatrix} 1 & 0 & 0 \end{bmatrix} \begin{bmatrix} q \\ \dot{q} \\ z \end{bmatrix}$$

$$when\ \dot{q} < 0$$

$$\begin{bmatrix} \dot{q} \\ \ddot{q} \\ \dot{z} \end{bmatrix} = \begin{bmatrix} 0 & 1 & 0 \\ \frac{-k}{m} & \frac{D_{rz}}{m} & -\frac{C_{rz}}{m} \\ 0 & B_{rz} & A_{rz} \end{bmatrix} \begin{bmatrix} q \\ \dot{q} \\ z \end{bmatrix} + \begin{bmatrix} 0 \\ \frac{1}{m} \\ 0 \end{bmatrix} F_e \tag{43}$$

$$y = \begin{bmatrix} 1 & 0 & 0 \end{bmatrix} \begin{bmatrix} q \\ \dot{q} \\ z \end{bmatrix}$$

$$G = Ac(g\rho L_{l,h} + P_{l,h}) \tag{44}$$

$$P_{l,h} = \int \frac{Ac\dot{q}}{C} \tag{45}$$

With the following properties of the State Space model

$A \in \mathbb{R}^{n*n}, B \in \mathbb{R}^{n*1}, C \in \mathbb{R}^{m*n}$ with $m \leq n$

3 Modelling of the pumping system

3.1 Explanation of the model

The entire model can basically be divided in to three steps:

1. $\dot{x}$ is calculated via (4) with as input matrices A and B. The calculated $\dot{x}$ will be integrated in order to obtain x. Matrices (A, As, B and Bs) will be switched depending on the velocities threshold of 0.
2. The 'integrated' state vector x is then multiplied with Matrix C in order to obtain each of the states. This is done for all of the states separately in order to let these states be the input for the matrices A and B again.
3. The energy of the pump is a function of the pressure source of the hydraulic system, area of the pistons and the velocity of the pistons. This function was difficult to express in a single Simulink block, therefore it was split into two parts. First the pressure source of the hydraulic system was calculated, after which this value was a component in the calculation of energy.

   The energy of the pumping system is derived based upon (Barradas-Berglind et al.,2017), this means that if the velocity inside the pistons is positive the energy should be expressed as

$$E_p = Ac\dot{q}P_s \tag{46}$$

   Furthermore, the power of the pump is zero if the velocity inside the pistons is negative or equal to zero

$$E_p = 0 \tag{47}$$

   The area of the pistons and the velocity of the pistons is calculated with the use of the mathematical model. The pressure of the source however needed adaption from the equation denoted in (31), the derivative of the coupling mechanism was needed to be implemented in this equation, because of the derivative of the flow rate in (31).

$$\dot{Q} = \dot{q}Ac \tag{48}$$

$$P_s = RAc\dot{q} - P_{l,h} - g\rho L_{l,h} + IAc\ddot{q} \tag{49}$$

3.1.1 Matrix A and it's in/outputs

The A-matrix is expressed by two different matrices and connected with the state variables to obtain the Ax part of the State Space representation. The two matrices are connected to the matrix multiplication because of the changing behaviour of the system under changing velocities of the pistons (see paragraph 2.6). The state variables are merged with the use of a vector condensate in order to feed the signal to the matrix multiplication. The output after the matrix multiplication is equal to Ax.

3.1.2 Matrix B and it's in/outputs

The B-matrix is expressed by two different matrices, in addition each of the matrices has a different input. The system is always under influence of the excitation data. However, provided that the velocity inside the pistons is positive the term G (gravitational influences) is also added to the input of the system. For that reason is a switch included to simulate this switching input behaviour. The gravitation influences is represented by (44). The gravitational influences is a function of the area of the pistons, gravitational constant, the density inside the water column, the length between both of the reservoirs and the pressure difference between the reservoirs. In this equation the pressure between both reservoirs changes over time. Therefore, this was needed to be calculated in a different matlab function with (30). All other elements inside this equation are a constant value in this research, therefore after including the pressure over time the function PTO_switching (see Appendix B) is able to calculate the Bu.

3.1.3 Matrix C and it's in/outputs

After Matrix A and B are multiplied to obtain $\dot{x}$, where after it will be integrated in order to obtain the state vector x again. The state vector will be multiplied by the matrix C, which differs for each state variable

$$C_q = [1\ 0\ 0] \tag{50}$$

$$C_{\dot{q}} = [0\ 1\ 0] \tag{51}$$

$$C_z = [0\ 0\ 1] \tag{52}$$

The radiation component z has size 24. Therefore, the matrix C has in fact a size of 26. This means that in $C_q$and $C_{\dot{q}}$ the final zero will be replaced with 24 zeros in a row.

The matrix C_z is arranged in a different way than the other two C matrices. This matrix will be represented by a sum of the identity matrix and two times a row being equal to 24 zeros. The exclusion of the velocity and the displacement is done by the summation of the rows, where after the inclusion of all 24 radiation components is done by the identity matrix in order to obtain all of the radiation values.

3.1.4 Energy of the pump

The energy of the pump can be divided into two main parts. First the Pressure Source will be calculated following (49), then this value can be used to calculate (46). The inputs of the Pressure source are given by the pressure difference between the reservoirs ($P_{l,h}$), the acceleration of the pistons ($\ddot{q}$) and the velocity of the pistons($\dot{q}$). These inputs will be multiplied according to (48) with its constant values. The acceleration of the pistons was calculated by the differentiation of the velocity.

The calculated Pressure Source is then fed into the Energy functions (PTO_energy3 and PTO_energy2)(see: Appendix A & B) along with the velocity of the pistons to be able to calculate (46). The energy is depended on the velocity of the pistons, the pump is not activated when the velocity inside the pistons is equal to zero. Therefore, a switch is included to simulate the pumping behaviour only when the velocity inside the pistons is equal to values above zero. The final results of the pumping system is the energy of the pump in Joules.

3.1.5 Potential Energy of the system

The potential energy is calculated based upon the hydraulic energy function of (Barradas-Berglind et al.,2017). This hydraulic energy function was derived with the use of a similar hydraulic system. Therefore, it is allowed to directly use the formulation of the Hamiltonian. The Hamiltonian is a function of the gravitational influences, the pressure and the dynamics of the pressure between the reservoirs. The only adjustment to the expression is the incorporation of the coupling mechanism. The coupling mechanism is given in (38).

The potential energy is expressed by

$$E_{pot} = \frac{1}{2} C\dot{P}^2 + I(Ac\dot{q})^2 + Cg\rho L_{l,h} P_{l,h} \tag{53}$$

All components which were needed to calculate the potential energy were already available in the mathematical model. The pressures and the velocity of the system needed to be fed into the function PTO_PotE using a vector condensate. All other components were known constants obtained from (Barradas-Berglind et al.,2017) and (Almuzakki et al.,2017).

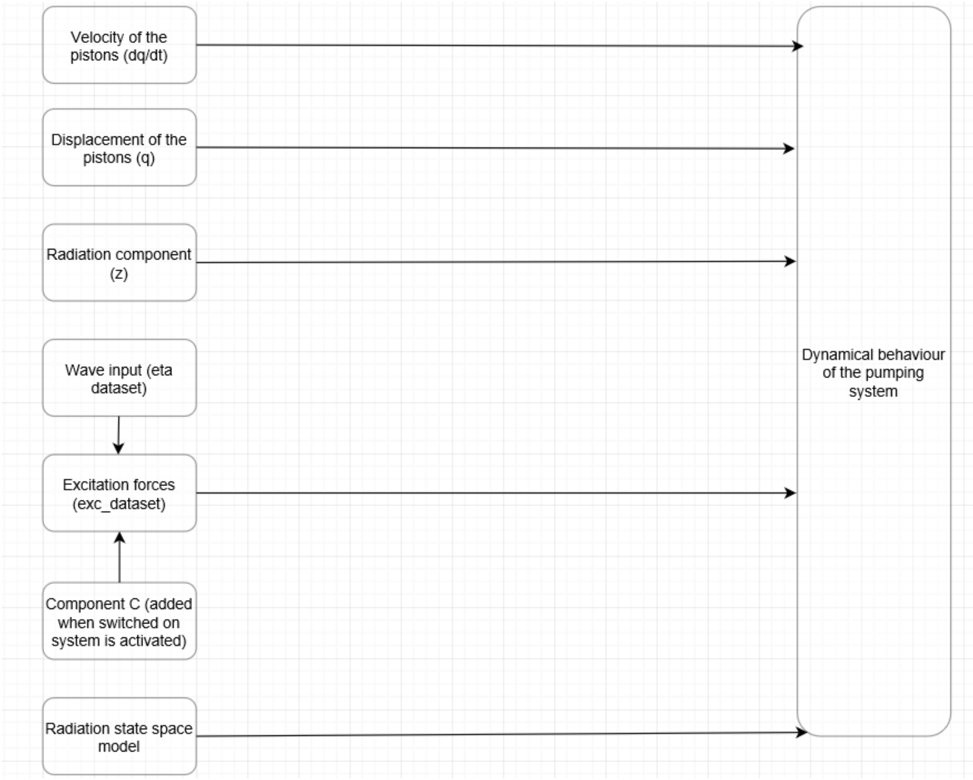

Figure 13: Conceptual model of all the different inputs to get to the dynamical behaviour of the pumping system.

3.2 Modelling an irregular wave

The modelling of the irregular wave was simplified because of previous researches of the Ocean Grazer Group. The research unit has already performed 7 years of research which generated a lot of usable datasets regarding the Ocean Grazer. In previous researches they obtained an substantial amount of datasets which can represents waves. These datasets are provided to researchers and students relevant to their work field. The irregular wave motion was however not directly fed in to the system. The wave motion was a one of the components in the excitation data which was also obtained from previous research. (see paragraph 2.3).

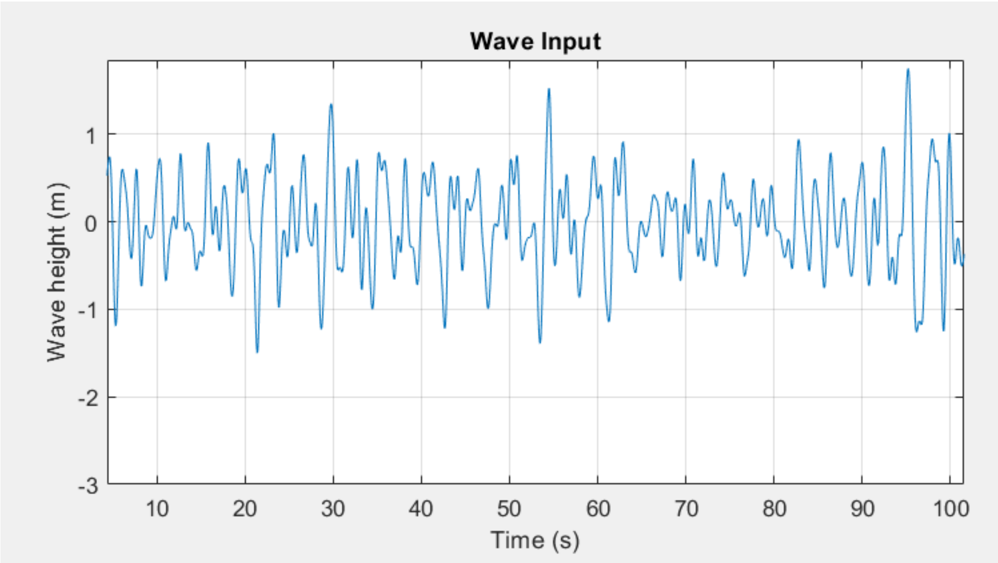

Figure 14: The Irregular Wave representation used in the mathematical model.

4 Simulations and results

4.1 Simulation parameters

The simulation done by the mathematical model was performed with some constant values or values which are obtained from previously mentioned equations. Most of the values taken in the research are comparable to (Barradas-Berglind et al.,2017) and (Almuzakki et al.,2017). In the table down below all the values taken in the research are listed.

Simulation Parameter	Value	units
Area Piston (Ac)	0.0738	m
Gravitational constant (g)	9.81	$\frac{m}{s^2}$
Length of the water column $(L_{l,h})$	100	m
Added Mass of the floater element (m_{∞})	101.68	kg
Mass of Floater element (m)	1500	kg
Area of the floater elements (Af)	49	m^2
Conditioned Fluid density inside the water column at 20°C (ρ)	998.2	$\frac{kg}{m^3}$
Fluid inertance at section water column (I_1, I_2)	338143.6	$\frac{kg}{m^4}$
Total fluid inertance system (I)	676287,2	$\frac{kg}{m^4}$
Fluid resistance at section (r_1, r_2)	102.67	$\frac{kg}{m^4 s}$
Total fluid resistance system (R)	205,34	$\frac{kg}{m^4 s}$
Fluid capacitance at section $(C_{h,r1}, C_{r2,l})$	200	$\frac{kg}{m^4 s^2}$
Total fluid capacitance system(C)	400	$\frac{kg}{m^4 s^2}$
Conditioned fluid dynamical viscosity (μ)	0.00089	$\frac{Ns}{m^2}$
Cross sectional area of the reservoirs (A_h, A_l)	49	m^2

Table 2: Simulation Parameters.

4.2 Validation of the results

The final results are given by the displacements of the pistons in the pumping system (q), the velocity of the pistons ($\dot{q}$), the behaviour of the pressure between the upper and lower reservoir over time, the energy of the pumping system and the energy stored in the higher reservoir.

The validation of the results will be based upon the expected outcome of the final results. The expected outcome is based upon the three reference papers used in this research, namely (Vakis et al.,2016), (Almuzakki et al.,2017) and (Barradas-Berglind et al.,2017). The latter paper has got the most correlation with this research and therefore the validation of the results will mainly be based upon this research.

The displacement of the pistons follows the behaviour of the wave input, this means that when the wave increases in height, the pistons inside the pumping system are working accordingly. Therefore, the conclusion can be drawn that there is a direct correlation between the wave input (fig.14) and the displacement of the pistons (fig.15).

The velocities inside the pistons (fig.16) match the expected behaviour of the displacement of the pistons (fig.15). When the displacement goes downwards, the velocity will become negative and vice versa. When looking at the possible velocities inside the piston, they have got representable values.

The pressure difference displayed in (fig.17) shows the same behaviour as in the research of (Barradas-Berglind et al.,2017). The pressure over the reservoirs is non-decreasing because of the accumulation of the conditioned fluid inside the upper reservoir. Moreover, the switching system influences the flow rate to an extend that it is never negative. Furthermore, this behaviour will influence the pumping energy.

The energy of the pump is displayed in (fig.18). The energy of the pump has got comparable values to the wave energy of the system displayed in (Vakis et al.,2016). The efficiency of the Ocean Grazer was previously calculated in (Vakis et al.,2016). In (Vakis et al.,2016) the calculated efficiency was above 98 %, which means that pump is very efficient. Thus, the energy of the pump should be comparable to the total energy per wave cycle calculated in (Vakis et al.,2016). Although, both researches used different wave motion and therefore should have different amount of energy per wave, the values give an approximation of the energy of a wave being used for Ocean Grazer energy calculations.

The potential energy is displayed in (fig.19). The behaviour of the potential energy is comparable to other research done by the Ocean Grazer Group. The potential energy is increasing over time because of the non-decreasing water level of the upper reservoir. Furthermore, the pumping behaviour can be direct correlated to the distribution of the potential energy over time. The potential energy remains equal when the pumping behaviour was negated due to negative velocity inside the pistons.

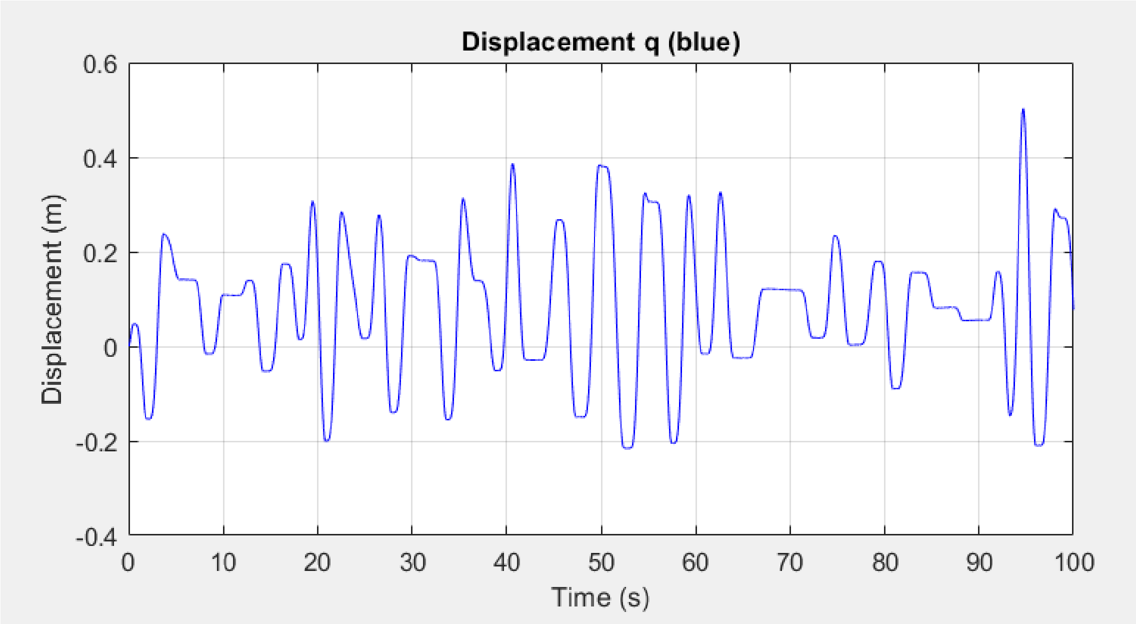

Figure 15: The displacement of the pistons inside the pumping system when the simulation is ran for 100 seconds.

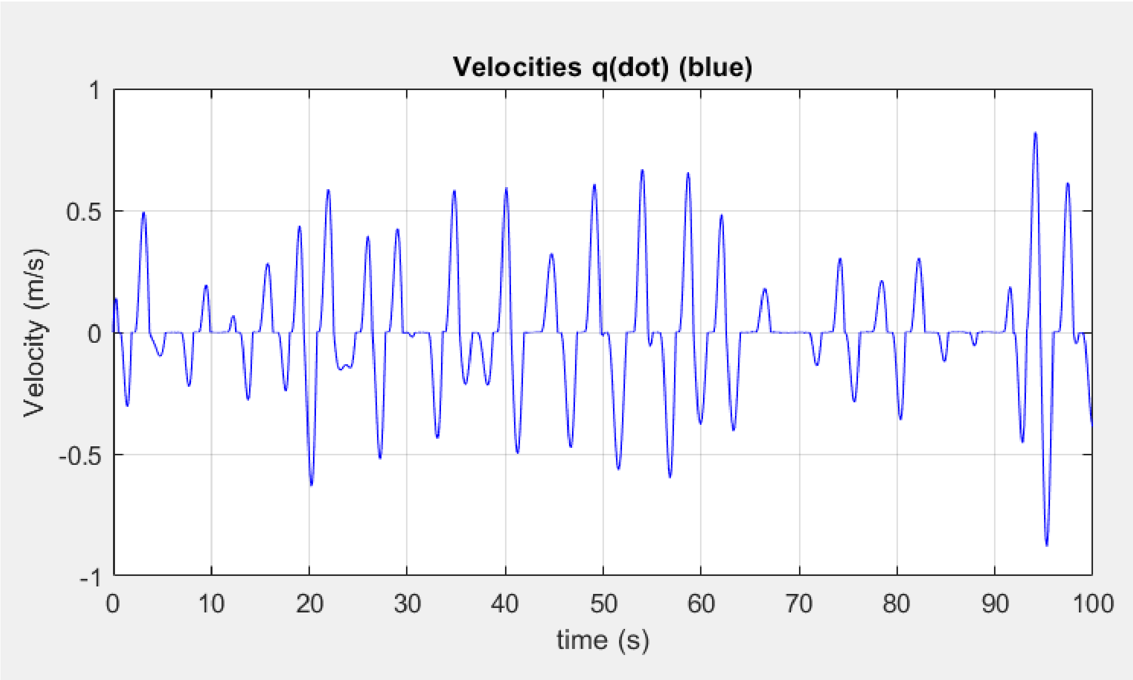

Figure 16: The velocities of the piston inside the pumping system when the simulation is ran for 100 seconds.

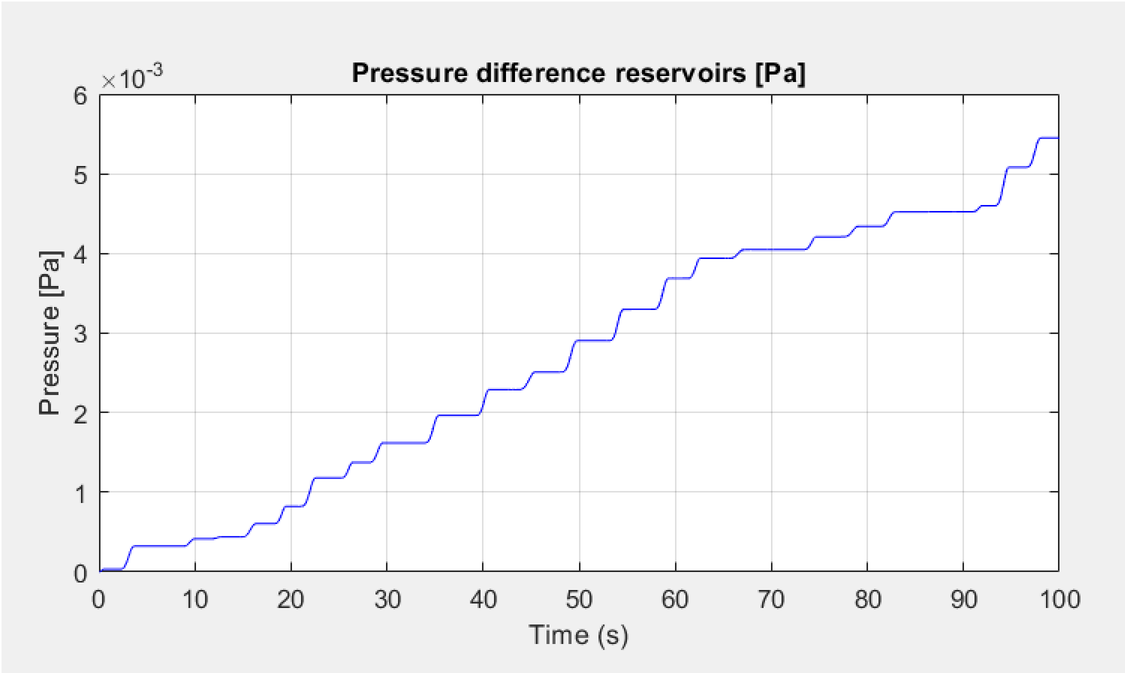

Figure 17: The pressure difference between the lower and higher reservoir when the simulation is ran for 100 seconds.

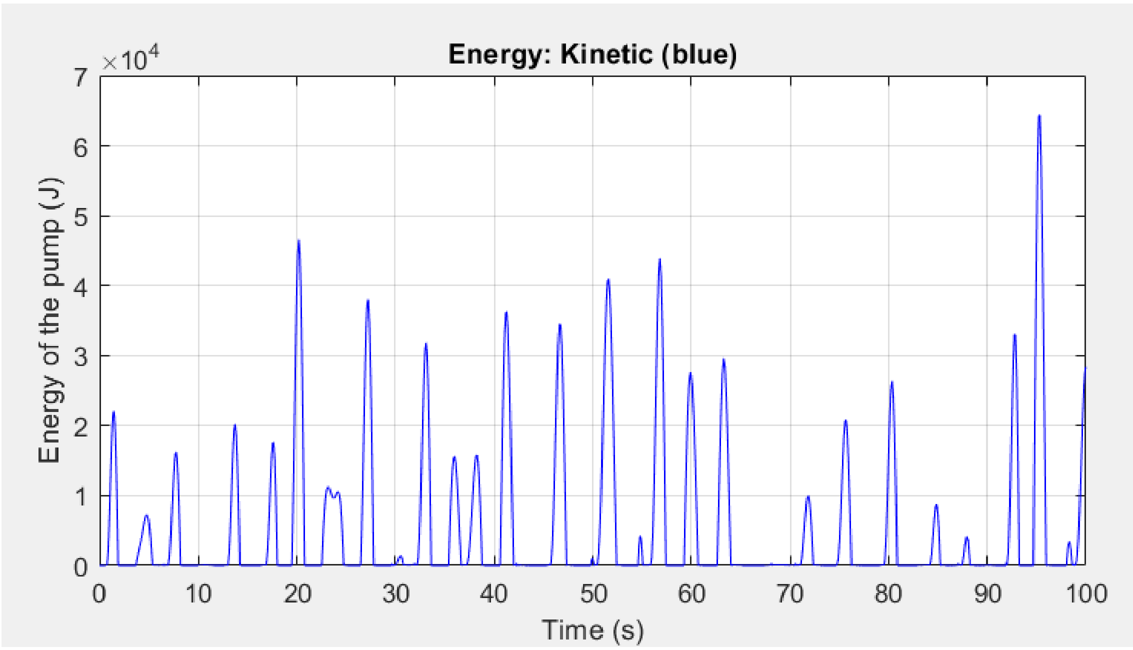

Figure 18: The energy of the pump on a simulation run of 100 seconds

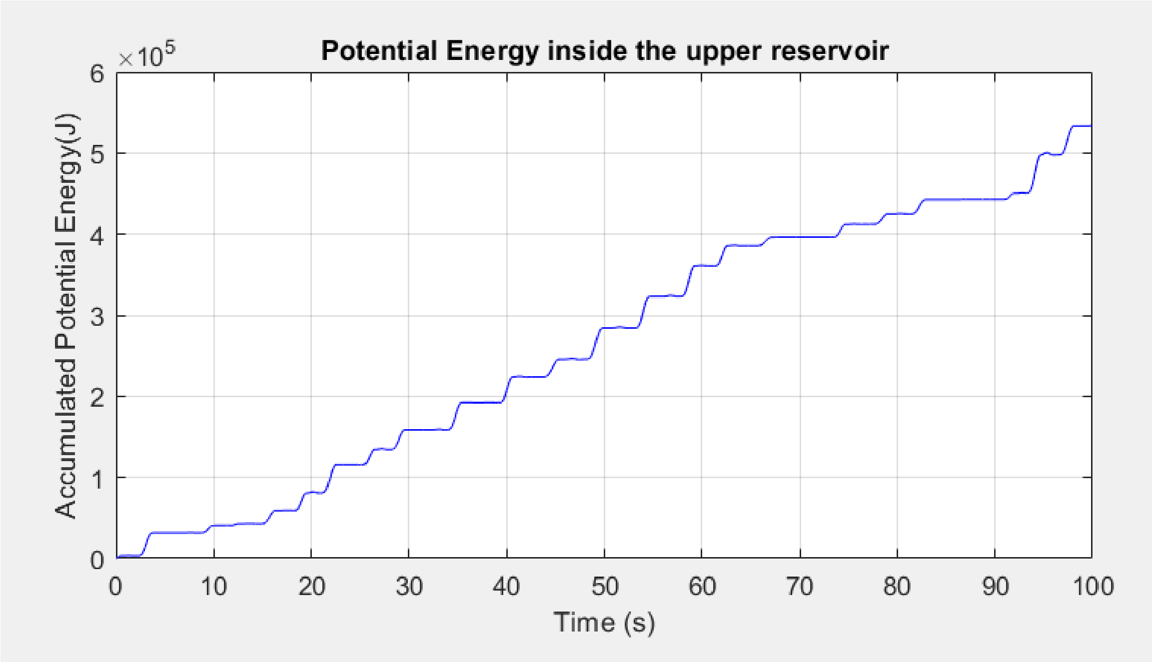

Figure 19: Potential Energy of the Ocean Grazer when the simulation is run for 100 seconds.

4.3 Comparison with simplified PTO

When comparing the results obtained from the simulation with (Barradas-Berglind et al.,2017) the following conclusions can be drawn. The overall behaviour of the pressure between both reservoirs is comparable, although the value in this simulation is higher due to the differences in displacement and velocities of the pistons especially on the time grid chosen for the simulations. In the early stages of the oscillations of the wave the displacements of the pistons are relatively low. This also explains the relatively low energy generation in the beginning of the simulations done with the non-linear wave input. Linear wave input achieves a constant energy output per wave cycle due to wave amplitudes being constant. In the new simulations the energy generation becomes higher after the wave displacement becomes higher. This relationship makes sense because bigger waves need to carry more mass which ultimately means that the waves carry more energy.

When the simulation is run for 800 seconds, the energy of the pump fluctuates between 30 KJ and 90 KJ. The expected energy per wave based upon (Vakis et al.,2016) is 99 KJ. The energy difference could be explained by the difference in inputs of the system, for example different areas of the pistons used but also different masses of the buoy-piston ensemble and the added mass of the system. The most obvious will be the different wave dynamics which could subsequently mean that the wave cycle used in this research has got lower energy per cycle. Because of limited time, the energy cycle of the eta.dataset(fig.14) is not yet investigated. Further research needs to be done to check how accurate the results are.

Other inconsistencies which could clarify some of the differences between this new research and (Barradas-Berglind et al.,2017) are the incorporated influences of radiation. Furthermore, although most of the parameters are chosen to be identical. The mass of the buoy and the added mass of the displaced water is chosen to be different. These values were based upon data from (Almuzakki et al.,2017).

This research uses different wave motion which influences the evaluated PTO force compared to(Vakis et al.,2016), also the radiation and excitation forces differ. Furthermore, the area of the pistons is taken to be a different constant.

5 Conclusion

In this report, a buoy-piston-pump point absorber system is investigated based upon the State Space approach. The hydraulic subsystem and mechanical subsystem are derived separately with the use of elemental equations where after both systems are coupled with a familiar coupling mechanism.

The coupled system is modelled within the Simulink and Matlab environment to see how the Ocean Grazers pumping system behaves under realistic wave motion compared to previous researches based upon linear simplifications of the wave motion which were used in previous research of the Ocean Grazer Group.

As expected, the pumping system will behave differently with a nonlinear power take off. But still, the differences regarding the output of the system, in terms of energy used by the pump are getting close to the overall energy output of a wave cycle (Vakis et al.,2016). Furthermore, the behaviour of the pressure differences between the reservoirs were similar to (Barradas- Berglind et al.,2017).

The potential energy is non-decreasing because of the increasing volume of water at an elevated level. The efficiency of the pump is not yet properly calculated because of the lack of information about the energy per wave cycle of the eta.dataset. Further research needs to be done in order to calculate the efficiency of the pumping system under realistic wave motion accurately.

To finalize, the behaviour of the pumping system was comparable to previous research which was represented with linear PTO, the main difference however is that the irregularity of the wave translates to the same irregular displacements of the pistons. The aforementioned irregularity will influence the energy generation of the pumping system. Instead of a constant output of energy, the energy fluctuates depending on the wave height and period, which is in line with linear PTO researches with changing wave heights and periods.

6 Recommendations for future research

The simulations and results are bounded to some assumptions, for example the influences of the third subsystem on the energy output is not incorporated. The relationship between the hydraulic and mechanical subsystem in comparison to the energy generating subsystem is neglected in this research. Further research could focus into the relationship between the energy generated subsystem and the scope of this research (hydraulic + mechanical subsystem). This can generate the overall power output of the Ocean Grazer when considering one single output such that an better estimation of the energy output can be researched.

Secondly, I recommend to model the pumping system with the incorporation of more floater elements. In this research, the excitation data of the first floater of the ten floaters considered in the Research of Almuzakki and R.J.Boer was used. In theory, all ten floaters could be considered in further research of the pumping system of the Ocean Grazer. However, the State Space representation for that research will be different then the State Space representation considered in paragraph 2.6.

In this research the area of the pistons is considered to be a constant value where in reality the area of the pistons can adapt to the energy of the wave such that the energy extracted from the incoming wave will be maximized. The Ocean Grazer has got the ability to switch to seven different piston areas. Due to limited time in this project it was impossible to set the area of the pistons to be variable depending on the wave energy. Future research could be based upon (Barradas-Berglind et al.,2016). In this research the pistons area was considered to be a control input. I recommend further focuses on implementing an alternative representation of the pistons area and model it within the Matlab and Simulink environment.

7 References

1. Shafiee, S. and Topal, E. (2009). When will fossil fuel reserves be diminished?. *Energy Policy*, 37(1), pp.181-189.
2. Pérez-Lombard, L., Ortiz, J. and Pout, C. (2008). A review on buildings energy consumption information. *Energy and Buildings*, 40(3), pp.394-398.
3. Drew, B., Plummer, A. and Sahinkaya, M. (2009). A review of wave energy converter technology. *Proceedings of the Institution of Mechanical Engineers, Part A: Journal of Power and Energy*, 223(8), pp.887-902.
4. Emec.org.uk. (2018). *Wave devices : EMEC: European Marine Energy Centre*. [online] Available at: http://www.emec.org.uk/marine-energy/wave-devices/ [Accessed 16 May 2018] (addition of 3).
5. Barradas-Berglind, J., Muñoz-Arias, M., Wei, Y., Prins, W., Vakis, A. and Jayawardhana, B. (2017). Towards Ocean Grazer's Modular Power Take-Off System Modeling: a Port-Hamiltonian Approach. *IFAC-Papers Online*, 50(1), pp.15663-15669.
6. Almuzakki, M., Barradas-Berglind, J., Wei, Y., Muñoz-Arias, M., Vakis, A. and Jayawardhana, B. A port-Hamiltonian Approach to Cummins' Equation for Floater Arrays with Linear Power-Take Off Systems.
7. Oceangrazer.com. (2018). *Ocean Grazer - Ocean Grazer*. [online] Available at: http://www.oceangrazer.com/prev/technology/ocean-grazer [Accessed 19 May 2018].
8. Kulakowski, B., Gardner, J. and Shearer, J. (2009). *Dynamic Modeling and Control of Engineering systems*. 3th ed. Cambridge University Press, pp.61-65,219-244, 438-479.
9. Ocean Grazer 3.0. (2018). *Ocean Grazer 3.0 - Offshore renewable energy: Wind, Wave, and Storage*. [online] Available at: http://www.oceangrazer.com/ .
10. Oceangrazer.com. (2018). *Ocean Grazer - A novel ocean energy converter*. Available at: http://www.oceangrazer.com/prev/ .
11. Barstow, S., Haug, O. and Krogstad, H. (1998) Satellite Altimeter Data in Wave Energy Studies. Proc. Waves'97, ASCE, vol. 2, pp. 339-354.
12. Jacobson, M. (2009). Review of solutions to global warming, air pollution, and energy security. *Energy Environ. Sci.*, 2(2), pp.148-173.
13. Falnes, J. and Løvseth, J. (1991). Ocean wave energy. *Energy Policy*, 19(8), pp.768-775.
14. Kalman, R. and Kalaba, R. (1965). Linear system theory-The State Space approach. *Proceedings of the IEEE*, 53(9), pp.1282-1283.
15. Massel, S. (2013). *Ocean surface waves*. 2nd ed. World Scientific.
16. Hevner, A. (2007). A Three Cycle View of Design Science Research. *Scandinavian Journal of Information Systems*, pp.87-92.
17. van der Schaft, A. and Jeltsema, D. (2014). Port-Hamiltonian Systems Theory: An Introductory Overview. *Foundations and Trends® in Systems and Control*, 1(2), pp.173-378.
18. Young, I. (1999). *Wind Generated Ocean Waves*. 2nd ed. Elsevier, p.83.
19. Redstone.us.com. (2018). *Technical Readiness Level Scale | Redstone*. [online] Available at: http://redstone.us.com/technical-readiness-level-scale/[Accessed 22 May 2018].
20. Vakis, A. and Anagnostopoulos, J. (2016). Mechanical design and modeling of a single-piston pump for the novel power take-off system of a wave energy converter. *Renewable Energy*, 96, pp.531-547.
21. Rug.nl. (2018). *Catching waves | Science Linx News | Science LinX | University of Groningen*. [online] Available at: https://www.rug.nl/sciencelinx/nieuws/20140923_oceangrazer?lang=en [Accessed 16 Jun. 2018].
22. Barradas-Berglind, J., Prins, W., van Rooij, M., Clemente Pinol, S., Jayawardhana, B., Vakis, A., Galvan Garcia, B. and Meijer, H. (2016). Energy Capture Optimization for an Adaptive Wave Energy Converter. *Proceedings of the 2nd International Conference on Renewable Energies Offshore - RENEW 2016*, pp.1-8.
23. Yu, Z. (2017). Hydrodynamics analysis of floater blanket using boundary element method.

Appendix A Simulink model

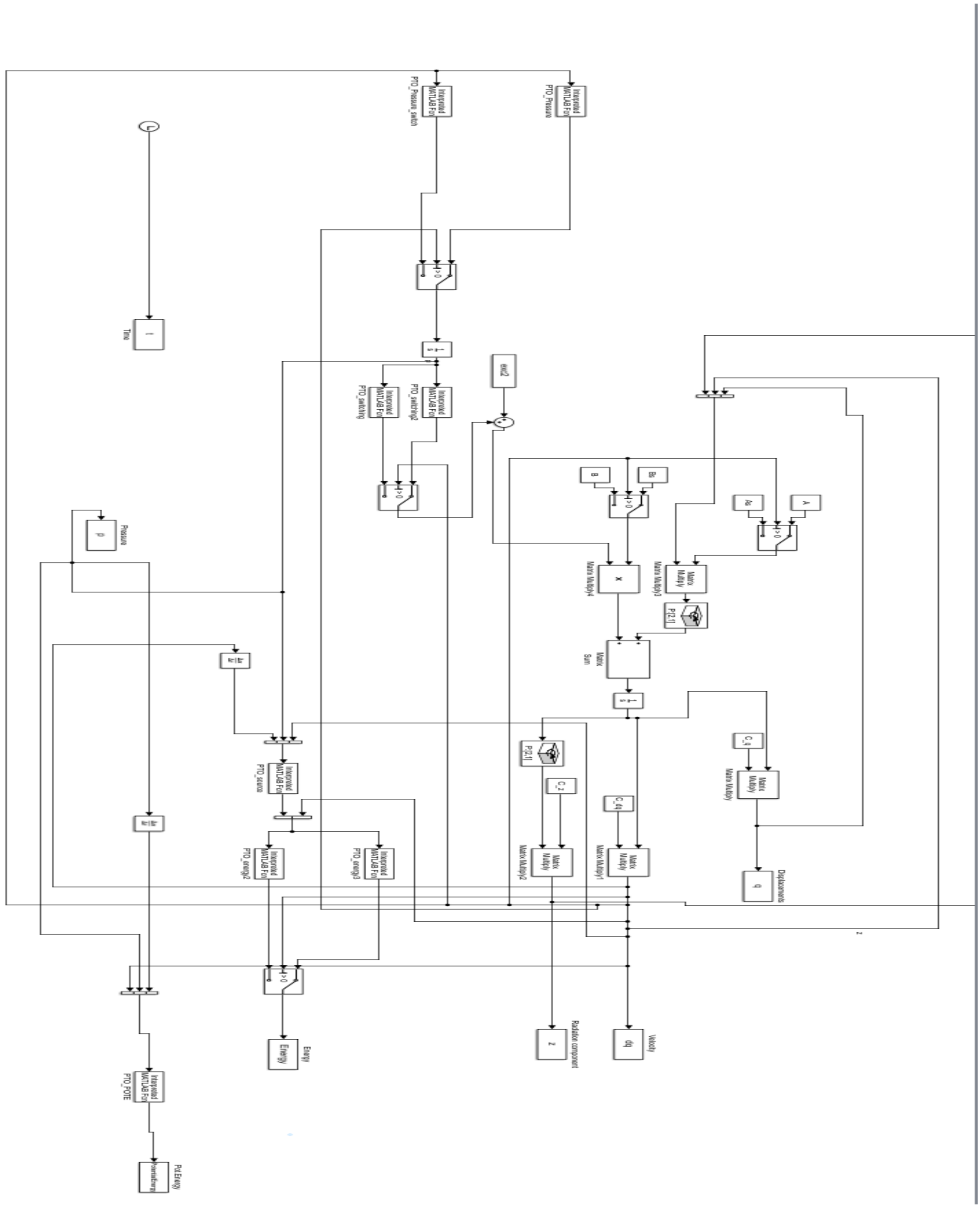

Figure 20: Simulink Model.

Appendix B Matlab codes used for simulink model

```
%State Space representation of the OG
%By Matthijs Loer
%7-June-2018
clc
clear all
close all
%
ZerosB = zeros(24,1);
C_z = [zeros(24,2) eye(24)];
C_q = [1 0 zeros(1,24)];
C_dq = [0 1 zeros(1,24)];

InitialC_PTO_dz = ZerosB;

    InitialC_PTO_q =0;


    InitialC_PTO_dq= 0;
    InitialC_PTO_dp=0;

    g   =  load('eta.mat');
    eta  = g.eta_data;
    eta2 = eta(:,2);

 %System Parameters
global Ac c
L = 100;
p = 998.2;
g = 9.81;
Ac = 0.0738;
m = 30*1500 + 101.882048780488;
Af = 49;
k = p * g * Af;
I12= 338143.6;
I56= 338143.6;
I= I12 + I56;
R23 = 102.67;
R45 = 102.67;
R = R23 + R45;
C13 = 200;
C46 = 200;
Ctotal= C13*C46 /(C13+C46);

C13 = 200;
```

```
C46 = 200;
c= C13*C46 /(C13+C46);
Eng=0.5*c;

 Ar = [-2.90489002260816,-3.49826263428946,-
1.13377593996359,-2.69079385969141,-
1.55057094938896,-2.39796313378942,-
1.22166795766577,-1.37265773439157,-
1.22721498569862,-2.11552442094118,-
1.64256455418795,-2.23571014618042,-
1.48619907062464,-1.61919691398318,-
0.902964621067619,-0.789230752111602,-
0.716085965205037,-0.995495371901553,-
0.698516338400689,-0.754969711395521,-
0.371842819727251,-0.597169251218832,-
0.320761348198424,-
0.348159558902095;16,0,0,0,0,0,0,0,0,0,0,0,0,0,0,0,0,
0,0,0,0,0,0,0;0,8,0,0,0,0,0,0,0,0,0,0,0,0,0,0,0,0,0,0
,0,0,0,0;0,0,4,0,0,0,0,0,0,0,0,0,0,0,0,0,0,0,0,0,0,0,
0,0;0,0,0,4,0,0,0,0,0,0,0,0,0,0,0,0,0,0,0,0,0,0,0,0;0
,0,0,0,4,0,0,0,0,0,0,0,0,0,0,0,0,0,0,0,0,0,0,0;0,0,0,
0,0,4,0,0,0,0,0,0,0,0,0,0,0,0,0,0,0,0,0,0;0,0,0,0,0,0
,4,0,0,0,0,0,0,0,0,0,0,0,0,0,0,0,0,0;0,0,0,0,0,0,0,2,
0,0,0,0,0,0,0,0,0,0,0,0,0,0,0,0;0,0,0,0,0,0,0,0,2,0,0
,0,0,0,0,0,0,0,0,0,0,0,0,0;0,0,0,0,0,0,0,0,0,2,0,0,0,
0,0,0,0,0,0,0,0,0,0,0;0,0,0,0,0,0,0,0,0,0,2,0,0,0,0,0
,0,0,0,0,0,0,0,0;0,0,0,0,0,0,0,0,0,0,0,2,0,0,0,0,0,0,
0,0,0,0,0,0;0,0,0,0,0,0,0,0,0,0,0,0,2,0,0,0,0,0,0,0,0
,0,0,0;0,0,0,0,0,0,0,0,0,0,0,0,0,2,0,0,0,0,0,0,0,0,0,
0;0,0,0,0,0,0,0,0,0,0,0,0,0,0,2,0,0,0,0,0,0,0,0,0;0,0
,0,0,0,0,0,0,0,0,0,0,0,0,0,1,0,0,0,0,0,0,0,0;0,0,0,0,
0,0,0,0,0,0,0,0,0,0,0,0,1,0,0,0,0,0,0,0;0,0,0,0,0,0,0
,0,0,0,0,0,0,0,0,0,0,1,0,0,0,0,0,0;0,0,0,0,0,0,0,0,0,
0,0,0,0,0,0,0,0,0,1,0,0,0,0,0;0,0,0,0,0,0,0,0,0,0,0,0
,0,0,0,0,0,0,0,1,0,0,0,0;0,0,0,0,0,0,0,0,0,0,0,0,0,0,
0,0,0,0,0,0,0.500000000000000,0,0,0;0,0,0,0,0,0,0,0,0
,0,0,0,0,0,0,0,0,0,0,0,0,0.500000000000000,0,0;0,0,0,
0,0,0,0,0,0,0,0,0,0,0,0,0,0,0,0,0,0,0,0.5000000000000
00,0];
 Br =
[32;0;0;0;0;0;0;0;0;0;0;0;0;0;0;0;0;0;0;0;0;0];

 Cr =
[2510.48763749122,410.858438600118,1022.71704957255,5
97.488905022445,1453.66704767529,753.262190047484,118
4.54327655013,540.012960292896,1223.61343345603,970.9
```

```
00760287191,1672.37476940909,1137.76165889473,1531.62
477112816,874.761947336797,931.121007846592,432.50382
7370248,727.258950110939,521.578317318424,682.7262885
34005,342.183608956786,337.102818562528,182.410264964
653,252.190027522984,0];

Dr = 0;

 A=[0 1 ZerosB';...
   -k/(m+I*Ac^2) (-R*Ac^2)/(m+I*Ac^2)-Dr/(m+I*Ac^2) -
Cr/(m+I*Ac^2);...
   ZerosB Br Ar];
As=[0 1 ZerosB';...
   -k/(m) -Dr/(m) -Cr/(m);...
   ZerosB Br Ar];

B = [0;...
  1/(m+I*Ac^2);...
  ZerosB];

Bs= [0;...
  1/(m);...
  ZerosB];


    load('newexcitation')


q=0;
dq=0;
z=ZerosB;

%%
Pto = sim('PTO','StopTime','800');
%%
q = Pto.get('q');
dq = Pto.get('dq');
t = Pto.get('t');
z = Pto.get('z');
Energy = Pto.get('Energy');
p = Pto.get('p');
%%

figure(1)
hold on
subplot(2,2,1)
plot(t,q(:,1),'b')
```

```
grid on
title('Displacement q_{1} (blue)')
xlabel('Time (s)')
ylabel('Displacement (m)')

subplot(2,2,2)
plot(t,dq(:,1),'b')
grid on
title('Velocities q(dot) (blue)','Interpreter','tex')
xlabel('time (s)')
ylabel('Velocity (m/s)')



% %  Plotting the energies

   subplot(2,2,3)
   plot(t,p(:,1),'b')
   grid on
   title('Pressure [Pa]')
   xlabel('Time (s)')
   ylabel('Pressure [Pa]')

  subplot(2,2,4)
  plot(t,Energy(:,1),'b')
  grid on
  title('Energy: Kinetic (blue)')
  xlabel('Time (s)')
  ylabel('Energy (J)')

  %%
  tx = size(t,1);
  figure(2)
  subplot(2,2,1)
  plot(t,exc2(1:tx,2),'b')
  grid on
  title('Excitation Force')
  xlabel('Time (s)')
```

- ```
  function [dx]= PTO_switching(p)
  ```

```
global Ac c
g=9.81;
rho=1035;
L=100;
dx= Ac*((g*rho*L)+p);
```

- ```
  function [dx]= PTO_switching2(p)
  ```

```
dx=0;
end
```

- ```
  function [dp]= PTO_Pressure(w)
  ```

```
dq= w(1);
global Ac c


dp = (Ac/c)*dq;
```

- ```
  function [dp]= PTO_Pressure_switch(w)
  ```

```
dq= w(1);
global Ac c


dp = 0*dq;

function [psource]= PTO_source(w)
```

```
dq= w(1);
P=w(2);
dqq=w(3);

L = 100;
p = 998.2;
g = 9.81;
Ac = 0.0738;
m = 30*1500 + 101.882048780488;
Af = 49;
k = p * g * Af;
I12= 338143.6;
I56= 338143.6;
I= I12 + I56;
R23 = 102.67;
R45 = 102.67;
R = R23 + R45;
C13 = 200;
C46 = 200;
Ctotal= C13*C46 /(C13+C46);

psource =R*Ac*dq-P-g*p*L + I*Ac*dqq ;


function [E]= PTO_energy2(w)

Ps=w(1);
dq=w(2);
Ac = 0.0738;


E =dq*Ac*Ps;


function [E]= PTO_energy3(w)

Ps=w(1);
dq=w(2);
E =0;


function [PE]= PTO_PotE(w)
```

```
dP=w(1);
P=w(2);
dq=w(3);
Ac = 0.0738;
g=9.81;
L=100;
rho=998.2;
I12= 338143.6;
I56= 338143.6;
I= I12 + I56;


C13 = 200;
C46 = 200;
Ctotal= C13*C46 /(C13+C46);


PE =0.5*Ctotal*dP+(Ac*dq)^2*I+Ctotal*g*rho*L*P;
```

Appendix C Current Ocean Grazer Group

Name	Function
Drs.W.A. Prins	Project manager
M.Van Rooij, MSc	Project leader
M.L.Greven	Secretary
Prof. Dr. Bayu Jayawardhana	Academic staff
Dr. Antonis Vakis	Academic staff
Y.Wei, PhD	Academic staff
M.Almuzakki, PhD	Research
M.Guo, PhD	Research
Industrial Engineering and Management students (BSc & MSc)	Research

Table 3: Members of the Ocean Grazer Group